Stephan C. Collins[1,2*,†], Hyun Woong Do[1*], Benoit Hastoy[1*], Alison Hugill[3*], Julie Adam[1], Margarita V. Chibalina[1], Juris Galvanovskis[1,4], Mahdieh Godazgar[1], Sheena Lee[4], Michelle Goldsworthy[3], Albert Salehi[5,6], Andrei I. Tarasov[1,7], Anders H. Rosengren[5], Roger Cox[3] and Patrik Rorsman[1,6,7]

Increased expression of the diabetes gene *SOX4* reduces insulin secretion by impaired fusion pore expansion

[1]OCDEM, Radcliffe Department of Medicine, Oxford OX3 7LJ, UK
[2]Université de Bourgogne Franche-comté
9E Boulevard Jeanne d'Arc 21000 France
[3]MRC Harwell, Mammalian Genetics Unit, Harwell Campus, OX11 0RD, UK
[4]Henry Wellcome Centre for Gene Function, Department of Physiology, Anatomy, and Genetics, University of Oxford, Parks Road, Oxford, Oxon OX1 3PT, UK
[5]Lund University Diabetes Centre, Department of Clinical Sciences, Skåne University Hospital Malmö, Lund University, 20502 Malmö, Sweden
[6]Department of Neuroscience and Physiology, University of Göteborg, Box 430, 40530, Göteborg, Sweden
[7]Oxford National Institute of Health Research, Biomedical Research Centre, Churchill Hospital, Oxford OX3 7LJ, UK

*Co-first author

[†]Current address: Institut de Génétique et de Biologie Moléculaire et Cellulaire, Illkirch, France

Key words: type-2 diabetes, insulin, exocytosis, *Sox4*, *Stxbp6*

The authors declare no conflict of interest

Corresponding author: Stephan C. Collins, collinss@igbmc.fr

This article contains Supplemental Data online at http://diabetes.diabetesjournals.org/lookup/suppl/xxxxxxx.xxx

Abstract

The transcription factor Sox4 has been proposed to underlie the increased type-2 diabetes risk linked to an intronic SNP in *CDKAL1*. In a mouse model expressing a mutant form of Sox4, glucose-induced insulin secretion is reduced by 40% despite normal intracellular Ca^{2+} signalling and depolarization-evoked exocytosis. This paradox is explained by a 4-fold increase in kiss-and-run exocytosis (as determined by single-granule exocytosis measurements), in which the fusion pore connecting the granule lumen to the exterior only expands to a diameter of 2 nm that does not allow the exit of insulin. Microarray analysis indicated that this correlated with an increased expression of the exocytosis-regulating protein Stxbp6. In a large collection of human islet preparations (n=63), *STXBP6* expression and GIIS correlated positively and negatively with *SOX4* expression, respectively. Overexpression of *SOX*4 in the human insulin-secreting cell EndoC-βH2 interfered with granule emptying and inhibited hormone release, the latter effect was reversed by silencing of *STXBP6*. These data suggest that increased *SOX4* expression inhibits insulin secretion and increased diabetes risk by upregulation of *STXBP6* and an increase in kiss-and-run exocytosis at the expense of full fusion. We propose that pharmacological interventions promoting fusion pore expansion may be effective in diabetes therapy.

Summary: 198 words of 200 allowed

Main text: 3999 words of 4000 allowed

INTRODUCTION

Reduced glucose-induced insulin secretion (GIIS) is a hallmark of type-2 diabetes (1). This disease results from a complex crosstalk between lifestyle factors (like body weight and age) and genetics (1). Insulin is released by Ca^{2+}-dependent exocytosis of insulin-containing secretory granules. Exocytosis involves the fusion of the granular membrane with the plasma membrane, a process that is initiated by the establishment of a narrow fusion pore connecting the granule lumen with the extracellular space (2). Effective release of insulin requires the rapid expansion of the fusion pore so that the secretory granules integrate with the plasma membrane.

Genome-wide association studies have led to the discovery of >100 loci associated with increased type-2 diabetes risk (3; 4), many of which are believed to act through reduced β-cell mass or interference with insulin secretion (5). For most of these loci, gene annotation is only tentative and based on the proximity of the single-nucleotide polymorphism (SNP) to a certain gene (4). An intronic SNP in the *CDKAL1* gene (rs7756992) is associated with a 50% increase in the risk of type-2 diabetes (6-9). However, recent data indicate *CDKAL1* is not the causative gene (9) and that its effect is instead mediated by altered expression of a nearby gene encoding the transcription factor *SOX4* (10).

Here we show that increased *SOX4* expression is associated with reduced GIIS and elevated plasma glucose and that increased *SOX4* expression impedes the delivery of insulin into the extracellular space via increased expression of the exocytosis-regulating protein *STXBP6* (amisyn). Overexpression of amisyn promotes the stabilization of the fusion pore and locks it in a partially expanded state (2-3 nm)

(11). This prevents the exit of insulin from the granule lumen into the extracellular space and thus impairs insulin secretion.

RESEARCH DESIGN AND METHODS

Animal husbandry

Animal work was approved by the local and national authorities. Mice used were described previously (12) but are heterozygous for the *Sox4* mutation and were *Insr*$^{+/+}$. Mice were killed by cervical dislocation and islets isolated by liberase digestion and handpicking as previously described (13). Static and dynamic measurements of insulin secretion were performed as in (12). Insulin was measured using a mouse insulin ELISA kit (Millipore, Hertfordshire, UK).

Mouse microarray studies

Islets were isolated from 22-week old male wild-type and mutant mice (four animals per genotype) and RNA extracted using a RNeasy mini-kit (Qiagen) and validated using an Agilent 2100 bioanalyzer (Agilent Technologies). Labeled and fragmented cRNA was hybridized to the Affymetrix 430 2.0 whole mouse genome microarray and processed on an Affymetrix GeneChip Fluidics Station 450 and Scanner 3000 (Affymetrix).

Cell transfections, siRNA and secretion assays

The constructs coding for GFP-tagged mouse and human *Sox4* and *Stxbp6* were

purchased from OriGene Technologies (Rockville MD, USA). The Y123C mutation was introduced into mouse *Sox4* using QuikChange protocol (Agilent Technologies). INS-1 832/13 cells were transfected using Lipofectamine RNAiMAX (Life Technologies, Paisley, UK). The following siRNAs were used: ON-TARGETplus siRNA SMARTpool for Stxbp6 gene and ON-TARGETplus Non-Targeting Control siRNA (Thermo Scientific, Hemel Hempstead, UK). After 24h, the cells were co-transfected with human growth hormone (hGH) and either DsRed or GFP-tagged mouse *Sox4* or *Stxbp6* using GeneJuice (Merck Millipore, Nottingham, UK). Supernatants and cell pellets were collected and the amount of growth hormone was measured by using an hGH ELISA kit (Roche Diagnostics, West Sussex, UK). EndoC-βH2 cells (14) were transfected with Human specific ON-TARGETplus siRNA SMARTpools (Thermo Scientific, Hemel Hempstead, UK) for *STXBP6* and *SOX4* were used in siRNA knockdown experiments. siRNA and transfections were performed as described for INS1-832/13 cells. Quantitative analysis of gene expression was performed using QuantiFast SYBR Green PCR kit and gene specific QuantiTect Primer Assays (both from Qiagen). Expression was calculated using ΔCt method with GAPDH as a reference gene.

Intracellular calcium measurements

Intracellular calcium concentration ($[Ca^{2+}]_i$) was assessed in freshly isolated intact islets using a dual wavelength PTI system (PTI, Monmouth, USA) fitted on an inverted Zeiss microscope allowing ratiometric measurements using the probe fura-

2AM (Invitrogen, Paisley, UK) as described previously (15).

Whole-cell measurements of Ca^{2+} currents and exocytosis

For patch-clamp measurements, islets were dissociated into single β–cells. In whole-cell measurements, insulin-secreting β-cells were identified based on their larger size (>5.5 pF) and complete inactivation of the Na^+ current at -70 mV (see ref. no (16)). Exocytosis and whole-cell Ca^{2+} currents were recorded using an EPC-10 amplifier and the Pulse software (Heka Electronics, Lamprecht/Pfalz, Germany) as described previously (15). Single exocytotic events and fusion pore expansion were detected in the cell-attached configuration. The standard extracellular solution described in (16) supplemented with 20 mM glucose was used as the pipette-filling medium. The PATCHMASTER software (Heka electronics) together with the EPC10 implements an 'internal calibration'. They automatically correct for phase-shifts and frequency-dependent attenuation when a sinusoidal voltage command of 25 kHz is generated (17). The scaled apparent capacitance (Im/ω) and conductance (Re) are then calculated online by the software.

$P2X_2$ receptor expression and current analysis

$P2X_2$ currents were recorded in the whole-cell configuration in identified β-cells as described previously (18,19). Experiments in EndoC-βH2 cells were performed after transfecting cells with both *STXBP6* as described above and $P2X_2$ receptors (as described in (20)). To evoke exocytosis, the cells were intracellular medium contained with 0-9 mM $CaCl_2$/10 mM EGTA mixture (calculated free $[Ca^{2+}]_i$: 0 or 2 μM), 3 mM

Mg-ATP and 0.1 mM cAMP. The current spikes reflecting vesicular release of ATP were analyzed using the Mini Analysis Program 6.0.3 (Synaptosoft, Decatur, USA) to determine the charge (integrated current; Q) and rise times ($t_{10\text{-}90\%}$) and half-widths (HW) of the individual events (20).

Electron microscopy

Isolated islets were washed in PBS and fixed in cold 2.5 % glutaraldehyde in PBS for 1h at 4°C and washed twice in PBS. Islets were incubated for 1h in 1% Osmium tetroxide and washed twice in PBS. Islets were dehydrated through an ethanol series for 5–10min each and then embedded in Agar 100 resin mix (Agar Scientific) pending sectioning and electron microscopy.

Human islet insulin secretion and microarray studies

Islets from cadaveric donors of European ancestry were provided by the Nordic Islet Transplantation Programme (http://www.nordicislets.org). All procedures were approved by the local ethics committee at Lund University. The islets were cultured in supplemented CMRL 1066 (ICN Biomedicals) for 1–9 days prior to RNA preparation. Total RNA was isolated with the AllPrep DNA/RNA Mini Kit (Qiagen). RNA quality and concentration were measured using an Agilent 2100 bioanalyzer (Bio-Rad) and Nanodrop ND-1000 (NanoDrop Technologies). Total RNA was converted into biotin-targeted cRNA, and the biotin-labeled cRNA was fragmented into strands with 35 to 200 nucleotides. This was hybridized onto a Affymetrix GeneChip® Human Gene 1.0 ST chip overnight in a GeneChip® Hybridization 6400 oven. The arrays were washed and stained in a GeneChip® Fluidics Station 450.

Scanning was carried out with the GeneChip® Scanner 3000 and image analysis was done with the GeneChip® Operating Software. Data normalization was performed using Robust Multi-array Analysis. Insulin secretion in human islets was measured as described previously (21). Microarray expression data have been deposited at GEO under the accession number GSE50398.

RESULTS

Impaired insulin secretion in *Sox4mt* mice

Mice harboring a point mutation (Y123C) in *Sox4* (*Sox4mt* mice) have previously been reported to be glucose-intolerant and hypoinsulinemic (12) but the precise mechanism by which this mutation results in diabetes is elusive. As shown in Figure 1*A-B*, islets from *Sox4mt* mice have reduced (-50%) GIIS over a range of glucose concentrations, despite similar insulin content, compared to wild-type (*Sox4wt*) islets. In dynamic (perifusion) measurements, both *Sox4wt* and *Sox4mt* islets responded to an elevation of glucose with a biphasic stimulation of insulin secretion (Fig. 1*C*) but GIIS was equally reduced at all times and the secretion defect could not be corrected by the K_{ATP} channel blocker tolbutamide (12).

Glucose-induced $[Ca^{2+}]_i$ increases, Ca^{2+} entry and exocytosis normal in Sox4mt β-cells

Insulin secretion is secondary to electrical activity and the associated elevation of cytoplasmic-free Ca^{2+} ($[Ca^{2+}]_i$) (22). We measured β-cell $[Ca^{2+}]_i$ in intact *Sox4wt* and *Sox4mt* islets (Fig. 2*A*). Both *Sox4wt* and *Sox4mt* islets responded to high glucose with

a marked, sustained and reversible increase in $[Ca^{2+}]_i$. Tolbutamide was equally effective at increasing $[Ca^{2+}]_i$ regardless of the genotype.

Since the reduction of insulin secretion in *Sox4mt* islets was neither corrected by tolbutamide, nor correlated with reduced $[Ca^{2+}]_i$, we hypothesized that the mutation instead interferes with insulin exocytosis (i.e. beyond the increase in $[Ca^{2+}]_i$). We thus compared insulin exocytosis in *Sox4wt* and *Sox4mt* β-cells by whole-cell capacitance measurements (23). Exocytosis was elicited by a train of depolarizations roughly emulating the bursts of action potentials that normally trigger insulin secretion (24). Surprisingly, the exocytotic responses were not reduced in *Sox4mt* β-cells (Fig. 2*B*). The magnitude of the voltage-gated Ca^{2+} currents in *Sox4mt* β-cells was the same as in *wt* cells (Fig. 2*C*), making it unlikely that an exocytotic defect is obscured by a compensatory increase Ca^{2+} entry.

Subtle effects on granule ultrastructure and number in Sox4mt β-cells

Ultrastructurally, *Sox4mt* β-cells appeared normal (Fig. *3A-B*) but the granule density was increased (Fig. 3*C*) whereas the dense core areas and granule diameters were marginally reduced (Fig. 3*D-E*).

Slow granule emptying in Sox4mt β-cells

The secretory granules of pancreatic β-cells store ATP together with insulin (25). We monitored single-granule release of ATP by infecting β-cells with an adenovirus encoding ionotropic purinergic $P2X_2$ receptors (26) (Fig. 4*A-B*). Exocytosis was triggered by intracellular application of high $[Ca^{2+}]_i$ (2 μM). Quantal (single-granule) release of ATP activates the $P2X_2$ receptors near the release sites and thus gives a rise

to transient membrane currents (19). The frequency of the exocytotic events thus detected was not different in *Sox4wt* and *Sox4mt* β-cells (0.24±0.04 and 0.24±0.04 events/s; not shown), in agreement with the whole-cell capacitance measurements of exocytosis (see Fig. 2*C*). Importantly, many of the current transients recorded in *Sox4mt* β-cells exhibited slower kinetics than those observed in *Sox4wt* cells (Fig. 4*C*). The size and shape of these transients reflect the amount and speed of ATP release (25). The charge (*Q*) and kinetics (rise times and half-widths) were measured as illustrated in Supplemental Figure 1**.** The cumulative histograms of the rise times in *Sox4wt* and S*ox4mt* β-cells are compared in Figure 4D. Whereas 70% of the events in *Sox4wt* β-cells had a rise time of <5 ms, 70% of the events in *Sox4mt* β-cells had rise times >5 ms. The events recorded in *Sox4mt* β-cells were also longer and the distribution of the half-widths was biphasic (Fig. 4*E*); ~20% of the events had duration of 50-200 ms (highlighted by arrow). However, no differences in the distribution of the charge (reflecting the total amount of ATP released) were detected (Fig. 4*F*).

Impaired fusion pore expansion in Sox4mt β-cells

We performed on-cell measurements of single-granule exocytosis and fusion pore conductance within the piece of membrane enclosed by the recording electrode. This technique allows fusion pore conductances to be measured for pores up to 10 nm in diameter (27) (Fig. 5*A*). In both *Sox4wt* and *Sox4mt* β-cells, stepwise increases in membrane capacitance (reflecting exocytosis of single insulin granules) were observed. The average amplitude of these steps was 5.2±0.5 (n=119) and 5.3±0.4 fF

(n=119). Assuming spherical geometry and a specific membrane capacitance of 10 $fF\mu m^{-2}$, these values correspond to a granule diameter of 0.4 μm, in reasonable agreement with the ultrastructural measurements (Fig. 3*E*). In *Sox4wt* β-cells, 88% of capacitance steps (Fig. 5*B*) were either associated with short-lived or no increases at all in membrane conductance (Fig. 5*A*, left), indicating rapid and irreversible expansion of the fusion pore and complete integration of the granule membrane with the plasmalemma (27). By contrast, in *Sox4mt* β-cells, 48% of capacitance steps often flickered between the baseline and an elevated level, as expected for 'kiss-and-run' exocytosis (28). This difference between *Sox4wt* and *Sox4mt* β-cells is statistically significant ($P=8.10^{-7}$ by χ^2 test). During these 'flickery' capacitance steps, persistent increases in membrane conductance were observed (Fig. 5*A*, right). The mean conductance increase averaged 340±31 pS (n=58). Assuming a cylindrical pore length of 15 nm (i.e. 2 x 7.5 nm; 7.5 nm being the thickness of a single membrane layer) and a solution resistivity of 66.7Ω.cm (equation 11.1 in (29)), this value corresponds to a fusion pore diameter of 1.8±0.2 nm (30). The cumulative distribution of the estimated fusion pore diameter is shown in Fig. 5*C*. In wild-type β-cells, the average fusion pore conductance and diameter were estimated to be 335±42 pS and 1.6±0.3 nm (n=14). It has been reported that the likelihood of kiss-and-run exocytosis correlates with granule diameter (29). We examined this aspect in Sox4mt β-cells. We found that capacitance increase associated with kiss-and-run exocytosis and full fusion averaged 6.3±0.7 (n=57) and 4.5±0.4 fF (n=62; $P<0.01$), respectively. This is opposite to what is expected from Laplace's law and argues that factors other than the diameter determines whether a granule undergoes kiss-and-run or full fusion exocytosis.

Gene expression microarrays

To identify target genes of *Sox4* in β-cells, we performed a gene expression microarray on *Sox4wt* and *Sox4mt* islets (Supplemental Table 2). A total of 60 genes were up-regulated (1.5- to 2.9-fold) and 56 genes were down-regulated (1.5- to 3.3-fold). Given the phenotype, genes involved in exocytosis are particularly interesting. These include *Stxbp6* (also known as amisyn; up-regulated 2.1-fold), *Doc2b* (down-regulated 1.8-fold) and *Rab3c* (down-regulated 2-fold). Total ablation of *Doc2b* was recently found to have only a small (10%) inhibitory effect on GIIS (30). Expression of a GTPase-deficient mutant of *Rab3c* has a very moderate effect on insulin secretion (31). Reduced expression of *Doc2b* and *Rab3c* are therefore unlikely to explain the reduction of GIIS in *Sox4mt* islets. However, overexpression of *Stxbp6* has been reported to slow the expansion of the fusion pore in adrenal chromaffin cells (11). The latter effect is obviously reminiscent of that we observe in *Sox4mt* β-cells.

Overexpression of *Sox4mt* interferes with glucose-induced secretion in rat insulinoma cells

In islets from *Sox4mt* mice, *Sox4* expression is increased by 100% compared to wild-type islets (Supplemental Fig. 3 in (12)). We therefore hypothesised that the effects on GIIS in *Sox4mt* islets may be mediated via increased Sox4 activity which, in turn, leads to increased *Stxbp6* expression and impaired fusion pore expansion. We compared the effects of similarly overexpressing *Sox4wt* and *Sox4mt* on *Stxbp6* expression in INS-1 832/13 cells (Supplemental Fig. 2). Both *Sox4wt* and *Sox4mt* increased *Stxbp6* expression, but the effect was stronger for the mutant (Fig. 6*A*). In

secretion experiments, down- and up-regulation of *Stxbp6* stimulated and inhibited glucose-induced growth hormone release (used as a proxy for insulin secretion in transfected cells (32)) by 30% and 40%, respectively (Fig. 6*B*). Whilst overexpression of *Sox4wt* had only a small inhibitory effect (-15%) on hormone release, stronger inhibition (-40%) was observed when overexpressing *Sox4mt* (Fig. 6*B*). Silencing *Stxbp6* largely reversed the inhibitory effect of overexpressing *Sox4mt*.

Increased SOX4 expression in human islets correlates with reduced GIIS

To extend these data to man, we correlated *SOX4* expression to donor HbA1c levels (a surrogate measure of long-term plasma glucose control), *STXBP6* expression and GIIS in a large collection of human islet preparations. There was a positive association between *SOX4* expression and HbA1c levels (Fig. 7*A*) and *STXBP6* expression (Fig. 7*B*) but a negative correlation between *SOX4* and GIIS (Fig. 7*C*). In agreement with published data (33), there was a tendency towards higher *SOX4* expression in islets from donors with type-2 diabetes (defined as established disease or HbA1c>6%; Supplemental Fig. 3*A*). There was also a positive association between *CDKAL1* and *SOX4* expression (Supplemental Fig. 3*B*).

These analyses suggest that increased *SOX4* expression, via elevated *STXBP6*, reduces GIIS in human β-cells. We confirmed this by experimentally up- and down-regulating *SOX4* and *STXBP6* in the glucose-responsive (Supplemental Fig. 3*C*) human β-cell line EndoC-βH2 (14). Moderate overexpression (+150%) of *SOX4* in EndoC-βH2 cells was associated with a 250% increase in *STXBP6* expression (Fig. 7*D*), an effect that was fully antagonised by knockdown of *STXBP6* by *siRNA* (*si-*

STXBP6). By contrast, silencing of *SOX4* did not reduce *STXBP6* expression below the low basal level. Overexpression of *SOX4* inhibited insulin secretion by 50%, an effect that was reversed by knockdown of *STXBP6* (Fig. 7*E*). Overexpression of *SOX4* also increased expression of syntaxin-1a (*STX1A*; Supplemental Fig. 3*D*), possibly to compensate for the binding of stxbp6 to syntaxin-1 (34), but this effect is unlikely to explain the suppression of insulin secretion as a positive correlation between *STX1A* expression and GIIS has been reported (35). Down-regulation of *SOX4* neither affected *STXBP6* expression (Fig. 7*D*), nor hormone release (Fig. 7*F*).

To examine the effect of increased *STXBP6* expression on granule emptying in human insulin-secreting cells, we expressed $P2X_2Rs$ in EndoC-βH2 cells and monitored single-granule ATP release (Fig. 7G). Overexpression of *STXBP6* resulted in a marked decrease in ATP release (measured as a decrease in *Q*; Fig. 7*H*). The mean charge of events was reduced by 90%. However, the frequency of the events was increased from 1.04±0.38 to 2.8±1.3 Hz (n=9 or 10; not statistically different). Combining the two effects suggest that there is a 70% reduction in stimulated ATP release following overexpression of *STXBP6* (Fig. 7I), in reasonable agreement with the 60% suppression of stimulated hGH release (Fig. 6B). Similar results were obtained in INS 832/13 cells. No ATP release events were observed when the EndoC-βH2 cells were infused with Ca^{2+}-free medium (Fig, 7F, top trace)

DISCUSSION

Type-2 diabetes represents an epitome of a polygenic disorder (1). Genome-wide association studies have led to the identification of ~120 common gene variants

(SNPs) with increased type 2 diabetes risk (36). For the majority of these gene variants, the precise cellular/molecular mechanisms underlying the increased disease risk remain obscure. The diabetes-associated SNP rs7756992 is commonly referred to *CDKAL1* but recently it was suggested that this locus increases disease risk via *SOX4* rather than *CDKAL1* (see (10)). Intriguingly, its expression is increased in diabetic islets (35) but whether increased expression of SOX4 is causally linked to type 2 diabetes and (if so) the underlying cell biological mechanism have not been studied.

Here we show that increased *SOX4* expression in human pancreatic islets correlates with reduced GIIS *in vitro* and increased HbA1C levels *in vivo*. Interestingly, we also found a correlation between *CDKAL1* and *SOX4* expression, in keeping with the idea that the *CDKAL1* locus influences the expression of both *CDKAL1* and *SOX4* (10). We also observed a tendency towards increased *SOX4* expression in islets from diabetic donors (Supplemental Fig. 3*A*), in agreement with what was previously reported based on microarray analysis of a β-cell-enriched fraction obtained my laser capture microdissection (35).

To address the mechanisms by which SOX4 may interfere with insulin secretion in man, we made use of the *Sox4mt* mouse model, in which islet *Sox4* expression is twice that of wild-type islet (12). We found that GIIS was reduced by ~50% in *Sox4mt* islets, a defect that was not corrected by the sulfonylurea tolbutamide. The reduction of insulin secretion could not be attributed to any impairment of key functional parameters such as glucose-induced $[Ca^{2+}]_i$, Ca^{2+} entry or exocytosis (determined as depolarization-evoked increases in whole-cell

membrane capacitance).

The delivery of insulin and other granule constituents, like ATP (25), into the extracellular space requires the establishment and expansion of a 'fusion pore' connecting the granule lumen and the exterior (27). Normally, the initial opening of the fusion pore is followed by its rapid expansion and, following a short delay, the entire granule 'collapses' into the plasma membrane, ensuring efficient delivery of the high molecular-weight cargo into the extracellular space ('full fusion'). Occasionally, however, fusion pore expansion is halted following the initial opening and may eventually close ('kiss-and-run' exocytosis (27)).

Using on-cell capacitance measurements of individual exocytotic events and the associated fusion pore openings, we found that full fusion was the predominant (~90%) form of exocytosis in *wt* β-cells, in agreement with previous reports (29). However, fusion pore expansion is impaired in *Sox4mt* β-cells and the fraction kiss-and-run release events increased to ~50% at the expense of full fusion. During the kiss-and-run events, the fusion pore is locked in a partially expanded state with a diameter of 1-2 nm.

We determined the functional impact of this on the evacuation of the granule lumen by measurements of ATP release. The molecular dimensions of ATP are 1.6*1.1*0.5 nm. With the observed distribution of fusion pore diameters, we estimate that ~20% of the total number of release events in *Sox4mt* β-cells (i.e. 43% of the 50% showing persistent fusion pore) have fusion pore diameters smaller/comparable to the narrowest cross-section of ATP (indicated by a vertical dashed line in Fig. 5C. Thus, the fusion pore may functions as a molecular sieve that restricts the exit of ATP

by steric hindrance. This likely accounts for the slower rise times of ATP release and the component of ATP release events with a duration >20ms (Fig. 4*D*). Larger molecules like insulin are likely to face an even greater problem exiting via the narrow fusion pore. At concentrations >2 mM, insulin exists as hexamer with a hydrodynamic radius of 5.6 nm (37). Given that the intra-granular insulin concentration is ≈100 mM (22), we conclude that insulin is trapped within the secretory granules undergoing kiss-and-run exocytosis. Indeed, the observed decrease in 'full fusion' from 88% to 52% is sufficient to account for the observed 40% reduction of GIIS in *Sox4mt* islets. It is tempting to speculate that the reduction in full fusion accounts for the increased granule density observed in *Sox4mt* β-cells. Although most fusion pores are mostly too small to allow exit of insulin, 10% have a diameter >6 nm. A fusion pore diameter as large as this is sufficient to allow the exit of a hexameric insulin, which might explain the slight reduction in dense core area of the insulin granules (Fig. 3*D*).

Being a transcription factor, it is not surprising that the expression of >100 genes were affected in *Sox4mt* islets. However, guided by the functional data implicating specifically kiss-and-run exocytosis, we identified *Stxbp6* (amisyn) as a likely mediator. Overexpression of *Stxbp6/STXBP6* mimics the effects of *Sox4/SOX4* on secretion in rat/human insulinoma cells. Conversely, silencing *Stxbp6/STXBP6* reverses the inhibitory effect of overexpressing *Sox4/SOX4*. Unexpectedly, and unlike what has previously been observed in rodent insulinoma cells (12), silencing *SOX4* in human insulinoma cells did not affect hormone release. The mechanism underlying this discrepancy remains unclear.

Our data suggest that increased expression/activity of *SOX4*, via increased expression of *STXBP6* and impaired expansion of the fusion pore, plays a role in insulin secretion and diabetes etiology. This scenario is in agreement with the proposal that Stxbp6 forms nonfusogenic complexes with syntaxin and thereby contributes to the regulation of SNARE complex formation (35). This is the first example of a major disease that can be linked to defective fusion pore expansion. It is possible that the mechanisms we have uncovered here may become activated during long-term hyperglycaemia, a condition reported to be associated with an increase in kiss-and-run exocytosis (38). It appears that the effect of increased *STXBP6* expression is graded. Whereas a moderate increase (up to +100%) results in an increased occurrence of kiss-and-run exocytosis (as seen in the Sox4mt mice), stronger overexpression may result in exocytosis being aborted before granule emptying (see Schematic in Supplemental Fig. 4). In cells overexpressing *STXBP6*, we observed small and short events, possibly reflecting repetitive openings/closures of the fusion pore releasing a puff of ATP every time.

If increased *SOX4* expression is part of the disease etiology and if it acts by interference with fusion pore expansion, then it may seem paradoxical that type-2 diabetes is not also associated with defects of neurotransmission. There is in fact a link between type-2 diabetes and neuropsychiatric disorders (39). It should be noted, however, that for low molecular-weight neurotransmitters, slowed/partial fusion pore expansion will only have a marginal effect on their release because they are small enough to pass through a constricted fusion pore.

This study illustrates how detailed cell physiological studies can help us move from SNPs, via identification of the actual gene involved, to a fuller understanding of the causal mechanisms. These findings raise the interesting possibility that pharmacological procedures promoting full fusion may correct the insulin secretion defect in type 2 diabetes.

Author Contributions. SC drafted, edited, revised the manuscript, prepared the figures, performed experiments, analysed the data and designed study. HD, BH, AH, drafted the manuscript, prepared the figures, performed experiments, analysed the data. JA, MC, JG, MG, AS, AHR, SL and AT performed experiments, analysed the data. RC and PR designed the study and drafted, edited, revised the manuscript. SC is the guarantor of this work and, as such, had full access to all the data in the study and takes responsibility for the integrity of the data and the accuracy of the data analysis.

Acknowledgements The authors acknowledge David Wiggins for technical assistance and the staff at the Mary Lyon Centre at MRC Harwell for maintaining the *Sox4* mutant mouse colony. Dr Patricia Muller (Leicester University) for advice on cell transfection, Professor Jochen Lang (Université de Bordeaux) and Professor Raphael Scharfmann (INSERM, Paris) for the provision of the INS-1 832/13 and EndoC-βH2 cells, respectively.

Funding The authors acknowledge support from the Wellcome Trust (Senior Investigator Award: 095531/Z/11/Z, PR), the Medical Research Council (BH, RC and PR, MR: /L020149/1),the Wellcome Trust-supported training programme OXION (JG), Swedish Research Council (VR, International Recruitment), and the Knut and Alice Wallenbergs Stiftelse (Wallenberg Scholars Programme).

Duality of Interest. No potential conflicts of interest relevant to this article were reported.

REFERENCES

1. Ashcroft FM, Rorsman P: Diabetes mellitus and the beta cell: the last ten years. Cell 2012;148:1160-1171
2. MacDonald PE, Braun M, Galvanovskis J, Rorsman P: Release of small transmitters through kiss-and-run fusion pores in rat pancreatic beta cells. Cell Metab 2006;4:283-290
3. McCarthy MI: Genomics, type 2 diabetes, and obesity. N Engl J Med 2010;363:2339-2350
4. Bonnefond A, Froguel P: Rare and Common Genetic Events in Type 2 Diabetes: What Should Biologists Know? Cell Metab 2015;
5. Rosengren AH, Braun M, Mahdi T, Andersson SA, Travers ME, Shigeto M, Zhang E, Almgren P, Ladenvall C, Axelsson AS, Edlund A, Pedersen MG, Jonsson A, Ramracheya R, Tang Y, Walker JN, Barrett A, Johnson PR, Lyssenko V, McCarthy MI, Groop L, Salehi A, Gloyn AL, Renstrom E, Rorsman P, Eliasson L: Reduced insulin exocytosis in human pancreatic beta-cells with gene variants linked to type 2 diabetes. Diabetes 2012;61:1726-1733
6. Zeggini E, Weedon MN, Lindgren CM, et al.: Replication of genome-wide association signals in UK samples reveals risk loci for type 2 diabetes. Science 2007;316:1336-1341
7. Scott LJ, Mohlke KL, Bonnycastle LL, Willer CJ, Li Y, Duren WL, Erdos MR, Stringham HM, Chines PS, Jackson AU, Prokunina-Olsson L, Ding CJ, Swift AJ, Narisu N, Hu T, Pruim R, Xiao R, Li XY, Conneely KN, Riebow NL, Sprau AG, Tong M, White PP, Hetrick KN, Barnhart MW, Bark CW, Goldstein JL, Watkins L, Xiang F, Saramies J, Buchanan TA, Watanabe RM, Valle TT, Kinnunen L, Abecasis GR, Pugh EW, Doheny KF, Bergman RN, Tuomilehto J, Collins FS, Boehnke M: A genome-wide association study of type 2 diabetes in Finns detects multiple susceptibility variants. Science 2007;316:1341-1345
8. Steinthorsdottir V, Thorleifsson G, Reynisdottir I, Benediktsson R, Jonsdottir T, Walters GB, Styrkarsdottir U, Gretarsdottir S, Emilsson V, Ghosh S, Baker A, Snorradottir S, Bjarnason H, Ng MC, Hansen T, Bagger Y, Wilensky RL, Reilly MP, Adeyemo A, Chen Y, Zhou J, Gudnason V, Chen G, Huang H, Lashley K, Doumatey A, So WY, Ma RC, Andersen G, Borch-Johnsen K, Jorgensen T, van Vliet-Ostaptchouk JV, Hofker MH, Wijmenga C, Christiansen C, Rader DJ, Rotimi C, Gurney M, Chan JC, Pedersen O, Sigurdsson G, Gulcher JR, Thorsteinsdottir U, Kong A, Stefansson K: A variant in CDKAL1 influences insulin response and risk of type 2 diabetes. Nat Genet 2007;39:770-775
9. Locke JM, Wei FY, Tomizawa K, Weedon MN, Harries LW: A cautionary tale: the non-causal association between type 2 diabetes risk SNP, rs7756992, and levels of non-coding RNA, CDKAL1-v1. Diabetologia 2015;
10. Ragvin A, Moro E, Fredman D, Navratilova P, Drivenes O, Engstrom PG, Alonso ME, de la Calle Mustienes E, Gomez Skarmeta JL, Tavares MJ, Casares F, Manzanares M, van Heyningen V, Molven A, Njolstad PR, Argenton F, Lenhard B, Becker TS: Long-range gene regulation links genomic type 2 diabetes and obesity risk regions to HHEX, SOX4, and IRX3. Proc Natl Acad Sci U S A 2010;107:775-780
11. Constable JR, Graham ME, Morgan A, Burgoyne RD: Amisyn regulates exocytosis and fusion pore stability by both syntaxin-dependent and syntaxin-independent mechanisms. J Biol Chem 2005;280:31615-31623
12. Goldsworthy M, Hugill A, Freeman H, Horner E, Shimomura K, Bogani D, Pieles G, Mijat V, Arkell R, Bhattacharya S, Ashcroft FM, Cox RD: Role of the transcription factor sox4 in insulin secretion and impaired glucose tolerance. Diabetes 2008;57:2234-2244
13. Shimomura K, Galvanovskis J, Goldsworthy M, Hugill A, Kaizak S, Lee A, Meadows N, Quwailid MM, Rydstrom J, Teboul L, Ashcroft F, Cox RD: Insulin secretion from beta-cells is affected by deletion of nicotinamide nucleotide transhydrogenase. Methods Enzymol 2009;457:451-480
14. Scharfmann R, Pechberty S, Hazhouz Y, von Bulow M, Bricout-Neveu E, Grenier-Godard M, Guez F, Rachdi L, Lohmann M, Czernichow P, Ravassard P: Development of a conditionally immortalized human pancreatic beta cell line. J Clin Invest 2014;124:2087-2098
15. Collins SC, Hoppa MB, Walker JN, Amisten S, Abdulkader F, Bengtsson M, Fearnside J, Ramracheya R, Toye AA, Zhang Q, Clark A, Gauguier D, Rorsman P: Progression of diet-induced

diabetes in C57BL6J mice involves functional dissociation of Ca2(+) channels from secretory vesicles. Diabetes 2010;59:1192-1201
16. Zhang Q, Chibalina MV, Bengtsson M, Groschner LN, Ramracheya R, Rorsman NJ, Leiss V, Nassar MA, Welling A, Gribble FM, Reimann F, Hofmann F, Wood JN, Ashcroft FM, Rorsman P: Na+ current properties in islet alpha- and beta-cells reflect cell-specific Scn3a and Scn9a expression. J Physiol 2014;592:4677-4696
17. Neef A, Heinemann C, Moser T: Measurements of membrane patch capacitance using a software-based lock-in system. Pflugers Arch 2007;454:335-344
18. Braun M, Wendt A, Karanauskaite J, Galvanovskis J, Clark A, MacDonald PE, Rorsman P: Corelease and differential exit via the fusion pore of GABA, serotonin, and ATP from LDCV in rat pancreatic beta cells. J Gen Physiol 2007;129:221-231
19. Obermuller S, Lindqvist A, Karanauskaite J, Galvanovskis J, Rorsman P, Barg S: Selective nucleotide-release from dense-core granules in insulin-secreting cells. J Cell Sci 2005;118:4271-4282
20. Karanauskaite J, Hoppa MB, Braun M, Galvanovskis J, Rorsman P: Quantal ATP release in rat beta-cells by exocytosis of insulin-containing LDCVs. Pflugers Archiv : European journal of physiology 2009;458:389-401
21. Rosengren AH, Jokubka R, Tojjar D, Granhall C, Hansson O, Li DQ, Nagaraj V, Reinbothe TM, Tuncel J, Eliasson L, Groop L, Rorsman P, Salehi A, Lyssenko V, Luthman H, Renstrom E: Overexpression of alpha2A-adrenergic receptors contributes to type 2 diabetes. Science 2010;327:217-220
22. Rorsman P, Renstrom E: Insulin granule dynamics in pancreatic beta cells. Diabetologia 2003;46:1029-1045. Epub 2003 Jul 1017.
23. Kanno T, Ma X, Barg S, Eliasson L, Galvanovskis J, Gopel S, Larsson M, Renstrom E, Rorsman P: Large dense-core vesicle exocytosis in pancreatic beta-cells monitored by capacitance measurements. Methods 2004;33:302-311.
24. Rorsman P, Eliasson L, Kanno T, Zhang Q, Gopel S: Electrophysiology of pancreatic beta-cells in intact mouse islets of Langerhans. Progress in biophysics and molecular biology 2011;107:224-235
25. Galvanovskis J, Braun M, Rorsman P: Exocytosis from pancreatic beta-cells: mathematical modelling of the exit of low-molecular-weight granule content. Interface Focus 2011;1:143-152
26. MacDonald PE, Rorsman P: The ins and outs of secretion from pancreatic beta-cells: control of single-vesicle exo- and endocytosis. Physiology (Bethesda) 2007;22:113-121
27. Alabi AA, Tsien RW: Perspectives on kiss-and-run: role in exocytosis, endocytosis, and neurotransmission. Annu Rev Physiol 2013;75:393-422
28. Hille B: Ion channels of excitable membranes Sunderland, Mass. , Sinauer, 2001
29. MacDonald PE, Obermuller S, Vikman J, Galvanovskis J, Rorsman P, Eliasson L: Regulated exocytosis and kiss-and-run of synaptic-like microvesicles in INS-1 and primary rat beta-cells. Diabetes 2005;54:736-743
30. Li J, Cantley J, Burchfield JG, Meoli CC, Stockli J, Whitworth PT, Pant H, Chaudhuri R, Groffen AJ, Verhage M, James DE: DOC2 isoforms play dual roles in insulin secretion and insulin-stimulated glucose uptake. Diabetologia 2014;57:2173-2182
31. Iezzi M, Escher G, Meda P, Charollais A, Baldini G, Darchen F, Wollheim CB, Regazzi R: Subcellular distribution and function of Rab3A, B, C, and D isoforms in insulin-secreting cells. Mol Endocrinol 1999;13:202-212
32. Dubois M, Vacher P, Roger B, Huyghe D, Vandewalle B, Kerr-Conte J, et al. Glucotoxicity inhibits late steps of insulin exocytosis. Endocrinology 2007 Apr;148(4):1605-14
33. Marselli L, Thorne J, Dahiya S, Sgroi DC, Sharma A, Bonner-Weir S, Marchetti P, Weir GC: Gene expression profiles of Beta-cell enriched tissue obtained by laser capture microdissection from subjects with type 2 diabetes. PLoS ONE 2010;5:e11499
34. Scales SJ, Hesser BA, Masuda ES, Scheller RH: Amisyn, a novel syntaxin-binding protein that may regulate SNARE complex assembly. J Biol Chem 2002;277:28271-28279
35. Andersson SA, Olsson AH, Esguerra JL, Heimann E, Ladenvall C, Edlund A, Salehi A, Taneera J, Degerman E, Groop L, Ling C, Eliasson L: Reduced insulin secretion correlates with decreased

expression of exocytotic genes in pancreatic islets from patients with type 2 diabetes. Mol Cell Endocrinol 2012;364:36-45
36. Prasad RB, Groop L: Genetics of type 2 diabetes-pitfalls and possibilities. Genes (Basel) 2015;6:87-123
37. Hvidt S: Insulin association in neutral solutions studied by light scattering. Biophys Chem 1991;39:205-213
38. Tsuboi T, Ravier MA, Parton LE, Rutter GA: Sustained exposure to high glucose concentrations modifies glucose signaling and the mechanics of secretory vesicle fusion in primary rat pancreatic beta-cells. Diabetes 2006;55:1057-1065
39. Gough SC, O'Donovan MC: Clustering of metabolic comorbidity in schizophrenia: a genetic contribution? J Psychopharmacol 2005;19:47-55

FIGURE LEGENDS

Figure 1- Impaired insulin secretion in *Sox4mt* islets. *A-B:* Insulin secretion *(A)* and content *(B)* measured in intact islets in static incubations. Islets were exposed to increasing glucose concentrations as indicated. Data are from 3 animals per genotype (with 3 technical replicates of 5 islets per animal) experiments. **P*<0.05. *C:* Dynamic measurements (perifusion) in *Sox4mt* (red) and *Sox4wt* (black) islets. Data are from 6 animals per genotype with 50 islets per animal and normalized to insulin content **P*<0.05 using a one-way Anova, repeated measures.

Figure 2- No impairment of $[Ca^{2+}]_i$ signaling, exocytosis (measured via whole cell capacitance) and Ca^{2+} currents. *A:* Glucose- and tolbutamide-induced increases in cytosolic Ca^{2+} in *Sox4wt (black)* or *Sox4mt* (*red*) islets. The glucose concentration was varied as indicated above the traces. Tolbutamide was added at a concentration of 0.2 mM. Traces are mean ± S.E.M. of 9 experiments for each genotype (3 islets per animal and 3 animals per genotype) and have been baseline corrected to correct for fading of the fluorophore. *B:* Increase in membrane capacitance (ΔC) during a train of ten 50 ms depolarizations from -70 mV to 0 mV (V) in *Sox4wt* (black) and *Sox4mt* (red) β-cells. Histogram (below) compares the total increase in membrane capacitance ($\Sigma\Delta C$) evoked by the train of depolarizations in *Sox4wt* (black) and *Sox4mt* (red) β-cells (n=24-28 β-cells from 4 mice per genotype). *C:* Peak current (I)-voltage (V) relationship for voltage-gated Ca^{2+} currents recorded from single *Sox4wt* (black) and *Sox4mt* (red) β-cells during depolarizations from -70 mV to membrane potentials

between -60 and +80 mV (n=13-16 β-cells from 4 mice per genotype). The horizontal dotted line indicates zero current level.

Figure 3- Subtle effects on cellular ultrastructure in *Sox4mt* β-cells. *A-B:* Representative electron micrographs from *Sox4wt* (*A*) and*Sox4mt* (*B*) β-cells. Scale bars: 1μm. *C-E*: Granule density (*C*) and box plots, depicting groups of data according to their quartiles, of the dense core area (*D*) and granule diameter (*E*) in *Sox4wt* (black) and *Sox4mt* β-cells (grey). At least 6 β-cells from 2 animals per genotype were analyzed. Data in (*D*) are mean ± S.E.M. ***P*<0.01. Distributions of core areas and granule diameters were estimated by counting >382 granules per genotype. **P<0.005; ***P<0.0005 (by Mann-Whitney U-test).

Figure 4- Delayed granule emptying in *Sox4mt* β-cells. *A*: Release of ATP monitored in individual *Sox4wt* β-cells expressing ionotropic $P2X_2$ receptors infused with 2 μM free $[Ca^{2+}]_i$. *B*: As in (*A*) but using from *Sox4mt* β-cells. Arrows indicate slow ('kiss-and-run') events. *C*: Rapid event recorded in a *Sox4wt* β-cell (black) and slow 'kiss-and-run' events recorded in a *Sox4mt* (red) β-cell. *D:* Cumulative histogram for the rise times in *Sox4wt* (black) and *Sox4mt* (red) β-cells. (*P*<0.005 by independent-samples Kolmogorov-Smirnov test). *E*: As in (*D*) for half-widths. The arrow indicates that ~20% of release events are of longer duration (*P*<0.005 by independent-samples Kolmogorov-Smirnov test). *F*: As in (*D-E*) for total charge (*Q*). Data shown in (*D-F*) based on >368 events obtained from 10 (*Sox4mt*) and 14 (*Sox4wt*) β-cells from 2 mice of each genotype. See also Supplemental Figure 1.

Figure 5- Impaired fusion pore expansion in *Sox4mt* β-cells. *A*: On-cell measurements of membrane capacitance (*C*) and conductance (*G*) showing two examples of full fusion (FF) from a *Sox4wt* β-cell (left) where the first event is associated with a prominent but short-lived increase in conductance (arrow) and an example of transient exocytosis (kiss-and-run; abbreviated KR) recorded from a *Sox4mt* β-cell (right) where *C* returns to baseline and the capacitance step is associated with a persistent increase in *G*. *B*: Pie charts summarizing the fraction of full fusion or kiss-and-run exocytosis in *Sox4wt* (n=119 events in 23 cells from 5 mice) and *Sox4mt* (120 events in 30 cells from 5 mice) β-cells ($P=8.10^{-7}$ by χ^2 test). *C*: Cumulative histogram of the distribution of estimated fusion pore diameters in *Sox4mt* β-cells. The dashed vertical line indicates a fusion pore diameter of 1.1 nm (enough to allow the exit of ATP). Also note that 10% of the events have an estimated pore diameter >6nm. See also Supplemental Table 1.

Figure 6- Mutant *Sox4* mediates its effects on insulin secretion via *Stxbp6*. *A*: qRT PCR analysis of *Stxbp6* expression in INS-1 832/13 cells transfected with scrambled siRNA + DsRed + hGH (dashed horizontal line; control), scrambled siRNA + *Sox4wt* + hGH (labeled '+*Sox4*') or scrambled siRNA + *Sox4mt* + hGH ('+*Sox4mt*'). †P<0.05 wt vs Sox4. *B*: hGH release (as a proxy for insulin release in transfected cells) from INS-1 832/13 cells transfected with scrambled siRNA + DsRed + hGH (labeled 'control'), *si-Stxbp6* + DsRed + hGH ('-*Stxbp6*') and scrambled siRNA + *Stxbp6* + hGH ('+*Stxbp6*'), scrambled siRNA + *Sox4wt* + hGH ('+*Sox4*'), *si-Stxbp6* + *Sox4wt* + hGH ('+*Sox4-Stxbp6*'), scrambled siRNA + *Sox4mt* + hGH ('+*Sox4mt*') and *si-Stxbp6* +*Sox4mt* + hGH ('+*Sox4mt-Stxbp6*') incubated with 1 or 20mM glucose (as indicated). Data are presented as mean ± S.E.M. of 4 experiments, each with 3 replicates. **P*<0.05; ***P*<0.01; and ****P*<0.001 for comparison vs control (1 or 20 mM glucose alone) and ††*P*<0.01 vs *Sox4wt* and ‡‡‡*P*<0.01 vs *Sox4mt* (by ANOVA and Tukey's tests). See also Supplemental Figure 2.

Figure 7- Effects of *SOX4* and *STXBP6* on human β-cell function. *A*: Relationship between *SOX4* expression and HbA1c levels. *R*=0.305; *P*=0.036; n=52. *B*: Relationship between *SOX4* expression and *STXBP6* expression *R*=0.321; *P*=0.021; n=63. *C*: Relationship between *SOX4* expression and GIIS. *R*=-0.292; *P*=0.043; n=48. For display, data in (*A-C*) have been grouped in quintiles. Best-fit black lines represent Pearson correlation analyses to the individual data points. *D*: qRT PCR analysis of *SOX4* and *STXBP6* expression in human cells transfected with scrambled siRNA + DsRed + hGH (dashed horizontal line; labelled 'Control'), scrambled siRNA + *SOX4wt* + hGH ('+*SOX4*'), *si-STXBP6* + *SOX4wt* + hGH ('+*SOX4-STXBP6*') and *si-SOX4* + DsRed + hGH ('-*SOX4*'). Data are presented as mean ± S.E.M. of 3 experiments, each with 3 replicates; **P<0.01 vs control (dashed horizontal line); ††*P*<0.01 vs '+*SOX4*' (by ANOVA and Tukey's tests). *E-F*: As in (*D*) but hGH release (as a proxy for insulin release in transfected cells) was measured in EndoC-βH2 cells exposed to 20mM glucose + 70mM [K^+]o. **P<0.01 vs 'control'; ††P<0.01 vs '+*SOX4*' (by ANOVA and Tukey's tests). Mean ± S.E.M. of 4 experiments, each with 3 replicates. Note that (*E*) and (*F*) were carried out independently, and for (*F*) data are presented as mean ± S.E.M. of 3 experiments, each with 3 replicates. See also Supplemental Figure 3A-D. *G*: Effects of overexpressing STXBP6 on ATP release in the human insulin-secreting cell line EndoC-βH2. Traces are labeled '*Control*' (cells expressing DsRed alone) and '+*STXBP6*' (cells overexpressing STXBP6). The top trace shows recordings when the cells were infused with Ca^{2+}-free medium (several sweeps have been superimposed). *H:* Cumulative histogram for the charge (*Q*) of the events in '*Control*' (black) and '+*STXBP6*' cells (red) (P<0.005 by independent-

samples Kolmogorov-Smirnov test). Data based on 1100-1400 events in 9-10 cells. *I*: Product of mean charge and frequency of events in '*Control*' and '+*STXBP6*' cells. $P<0.05$ vs. '*Control*'. See also Supplemental Fig. 4.

Figure-1 (Collins)

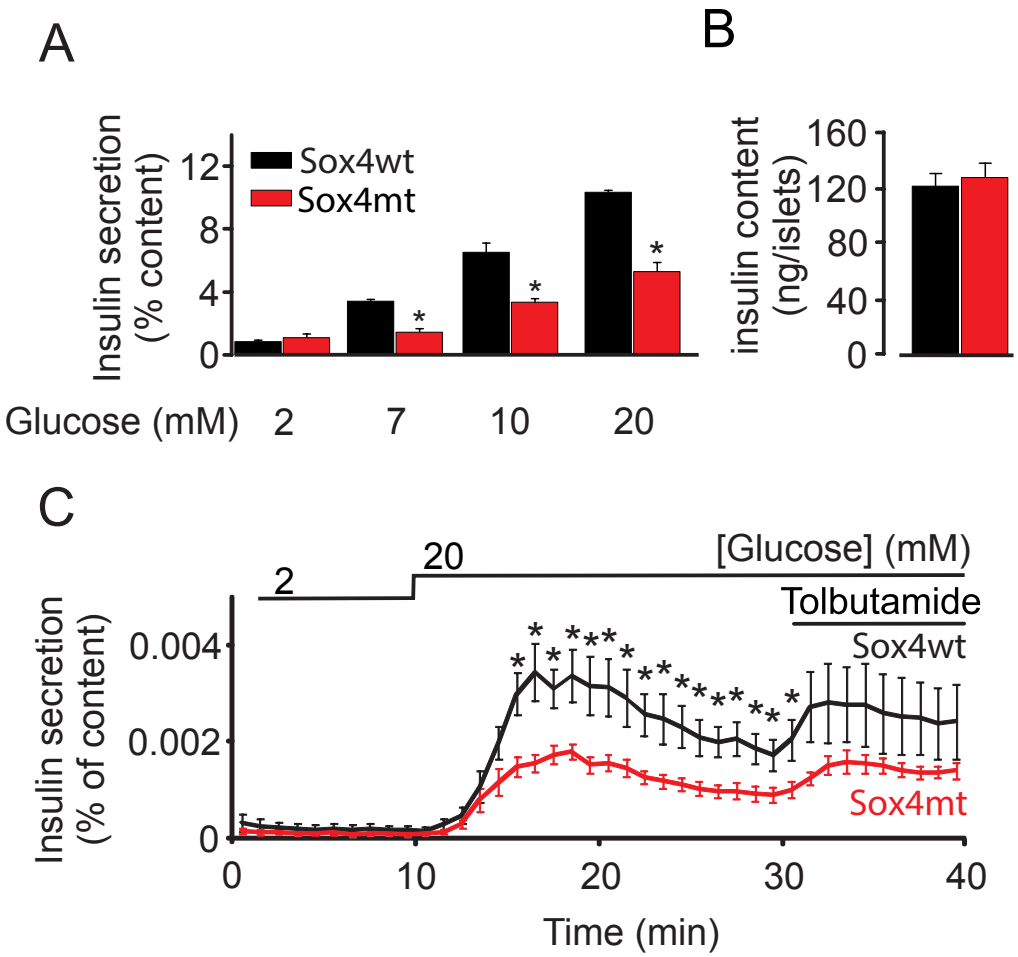

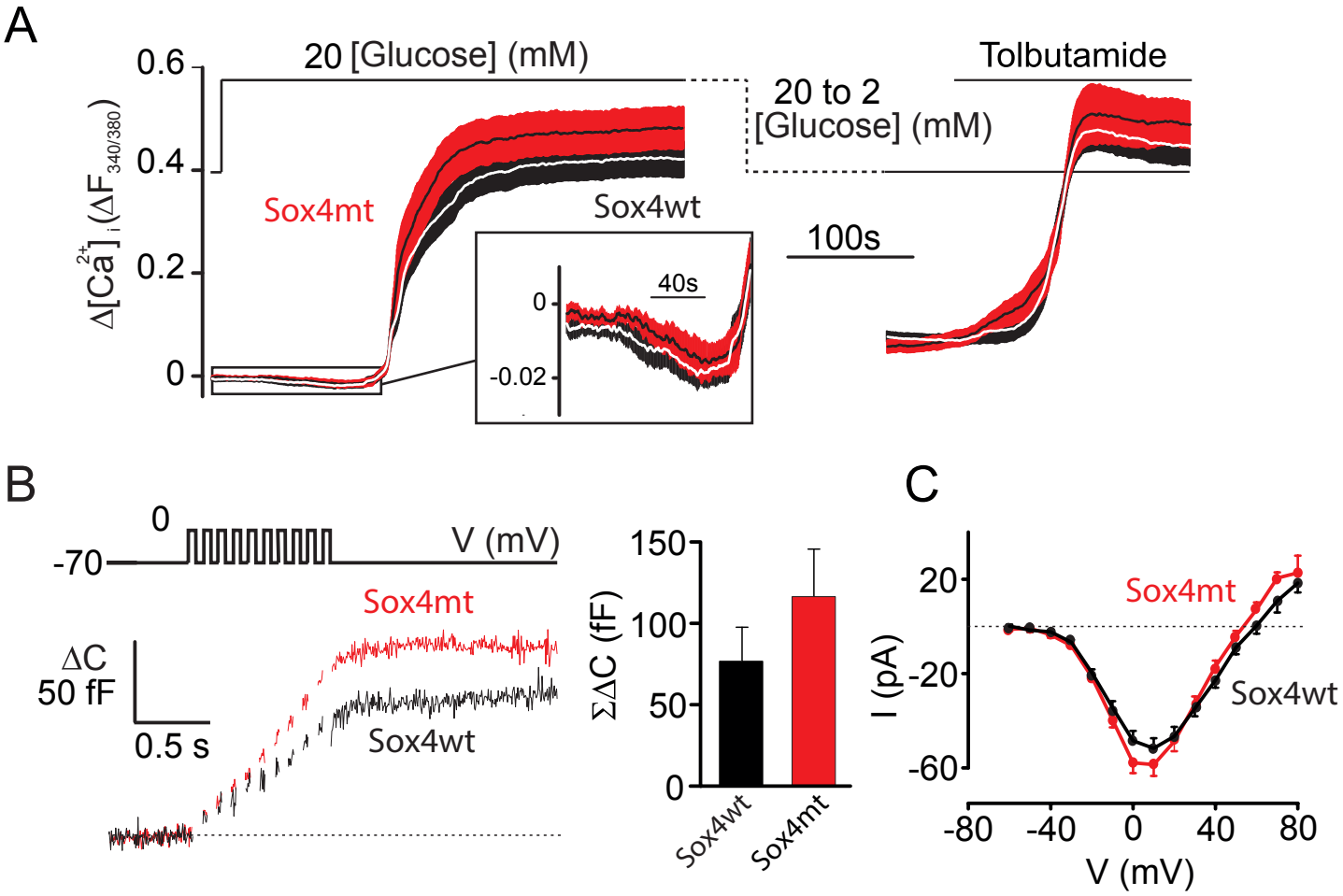

Figure-2 (Collins)

Figure-3 (Collins)

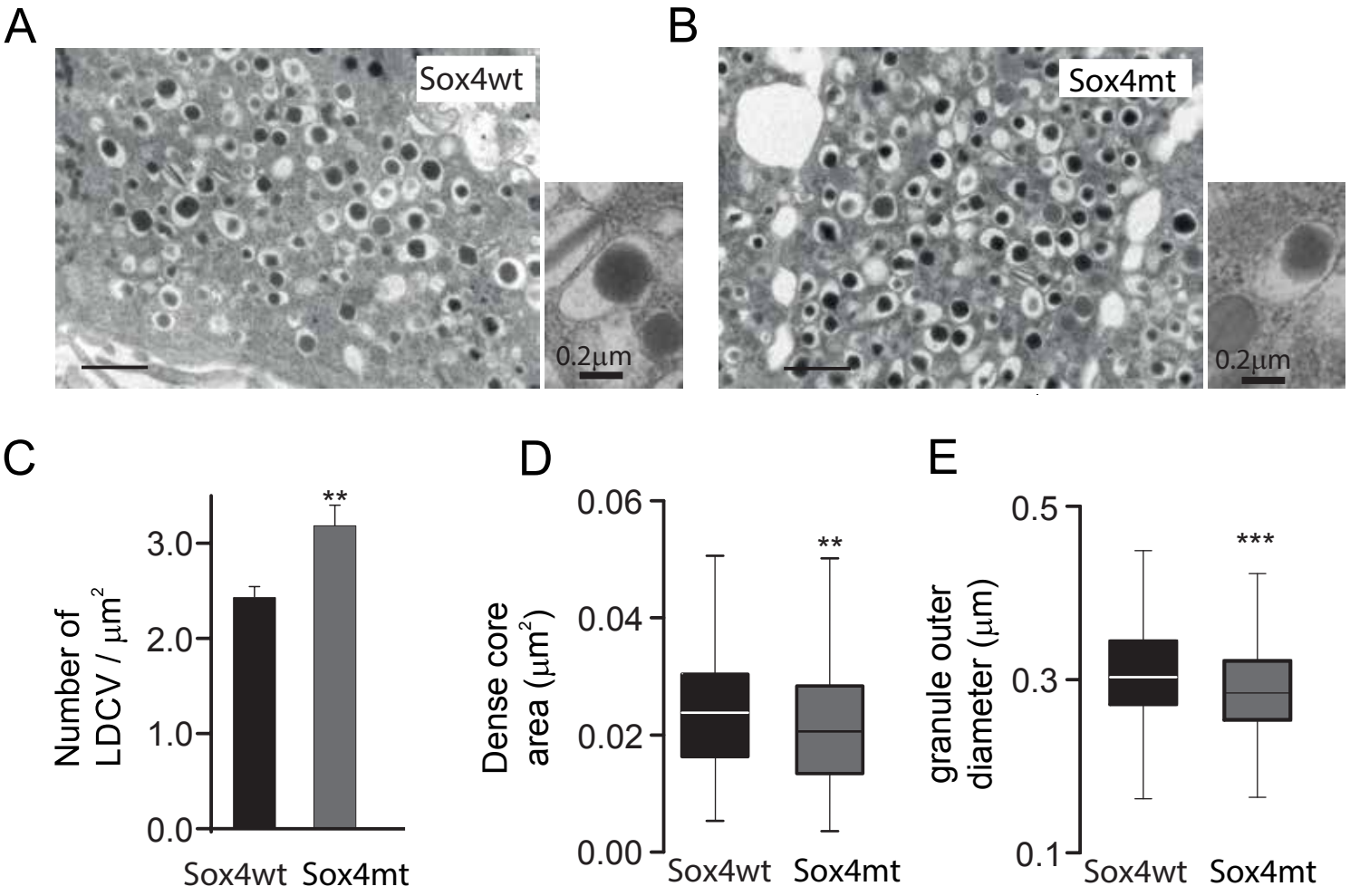

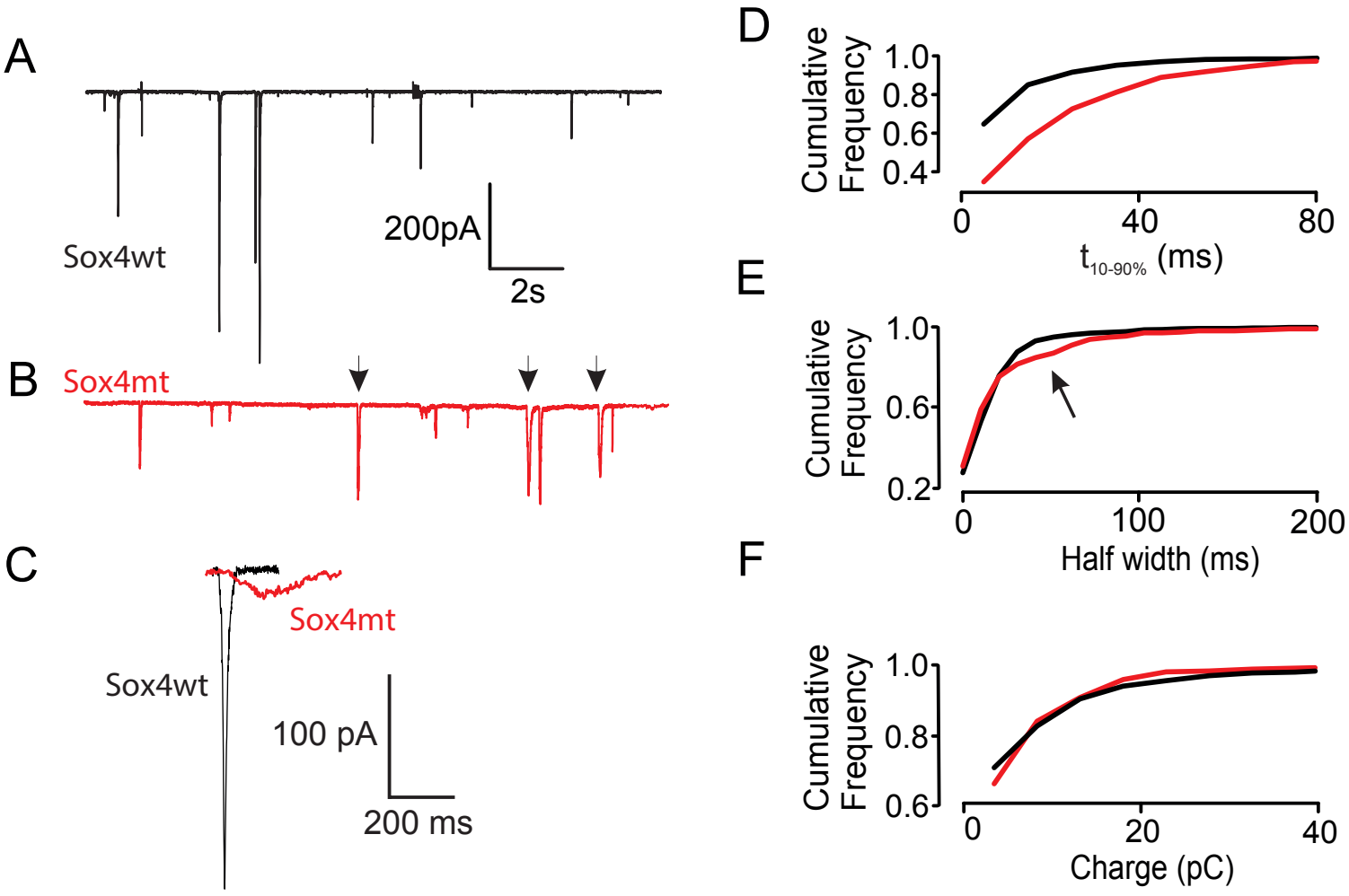

Figure-4 (Collins)

Figure-5 (Collins)

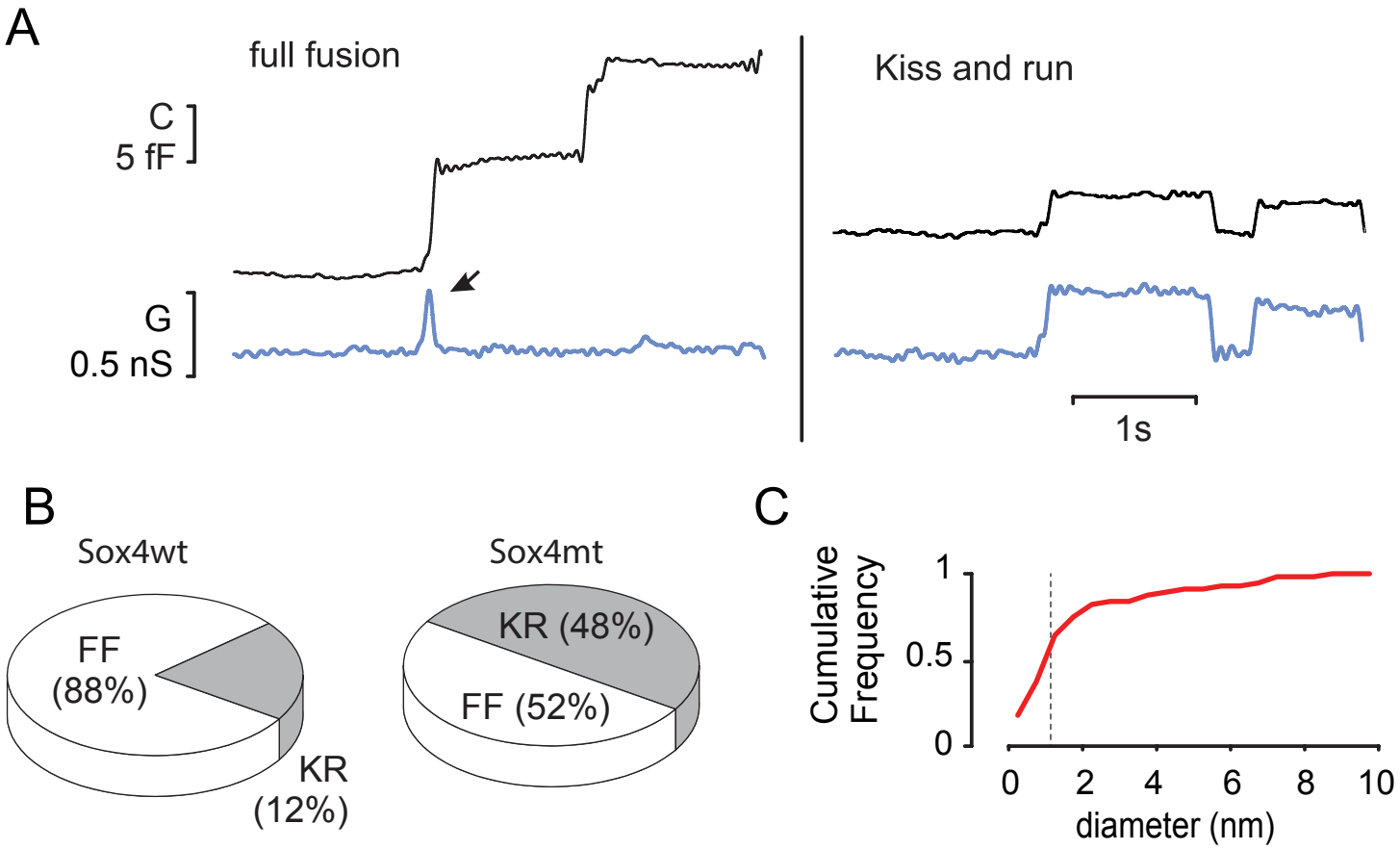

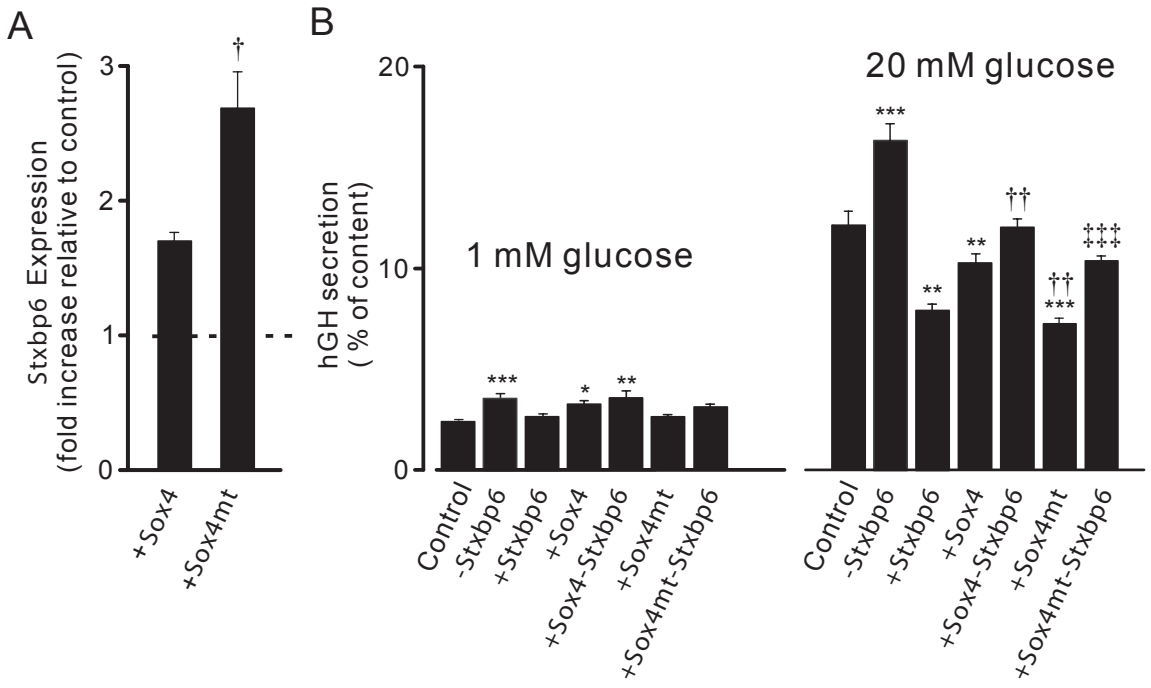

Figure-6 (Collins)

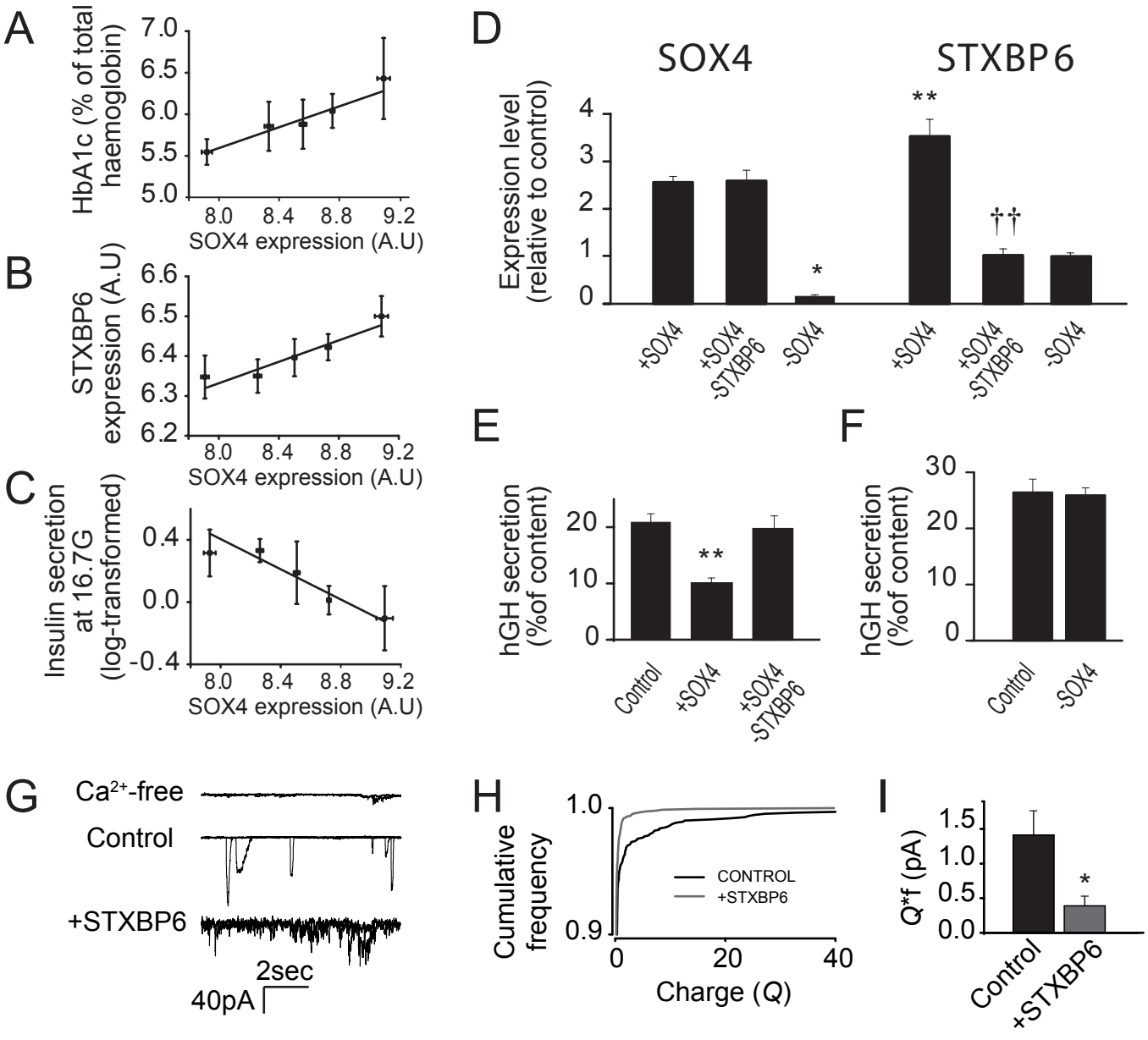

Figure-7 (Collins)

Stephan C. Collins, Hyun Woong Do, Benoit Hastoy, Alison Hugill, Julie Adam, Margarita V. Chibalina, Juris Galvanovskis, Mahdieh Gozdagar, Sheena Lee, Michelle Goldsworthy, Albert Salehi, Andrei I. Tarasov, Anders H. Rosengren, Roger Cox and Patrik Rorsman

Increased expression of the diabetes gene *SOX4* reduces insulin secretion by impaired fusion pore expansion

Justification for the requirement of the following supplemental material

Supplemental Table S1.

Full list of genes showing a significant ≥1.5 or ≤-1.5 fold expression change in *Sox4mt* islets.

Supplemental Figure S1.

Details how the $P2X_2$ current transient were analyzed and complements Figure 4D-E.

Supplemental Figure S2.

Levels of *Sox4wt* and *mt* expression achieved in a rat insulinoma cell line by transfection which serves as a control for Figure 6A.

Supplemental Figure S3.

(A-B) Focuses on expression data from human data sets and strengthens a role of SOX4 in human diabetes by supporting the previously published increased SOX4 expression in human diabetic islets (Supp. Fig. 3A) and reporting a positive correlation between *CDKAL1* and *SOX4* expression (Supp. Fig. 3B).

(C-D) characterizes the human beta cell line EndoC-βH2 and justifies the use of 20 mM G + KCl for stimulation in Figure 7E-F (Supp. Fig. 3C) and explores the expression of other exocytotic genes after *SOX4* overexpression (Supp. Fig. 3D).

Supplemental Figure 4.

Schematic explaining the relationship between STXBP6 expression and fusion pore expansion.

Supplemental Table 1. Effects of *Sox4mt* on gene expression.

GCRMA (Guanine Cytosine Robust Multi-Array Analysis) normalized differentially expressed genes with $P \leq 0.05$ (Welch t-test) and a ≥1.5-fold differential expression between *Sox4mt* and *Sox4wt* islets. Lists the genes with increased or reduced expression in Sox4mt islets. The microarray was carried out using RNA prepared from islets of 22-weeks old Sox4mt and Sox4wt mice (4 animals per genotype). Genes highlighted in red are involved in exocytosis

Fold increase	*P-value*	*Gene title*	*Gene name*
2.9	0.042	Gastrin	Gast
2.8	0.00311	RIKEN cDNA 6430502M16 gene	6430502M16Rik
2.4	0.0142	"deiodinase, iodothyronine, type I"	Dio1
2.4	0.0263	carboxypeptidase B2 (plasma)	Cpb2
2.2	0.0314	cell division cycle associated 8	Cdca8
2.2	0.0292	centromere autoantigen F	Cenpf
2.1	0.0304	topoisomerase (DNA) II alpha	Top2a
2.1	0.0222	apolipoprotein F	Apof
2.1	0.0207	syntaxin binding protein 6 (amisyn)	Stxbp6
2.1	0.00504	RIKEN cDNA4933405I11gene-mucin 4	4933405I11RikMuc4
2.0	0.0014	Expressed sequence BB164513	BB164513
1.9	0.0441	extracellular proteinase inhibitor	Expi
1.9	0.0234	antigen identified by monoclonal antibody Ki 67	Mki67 ///LOC638774
1.9	0.0438	shugoshin-like 1 (S. pombe)	Sgol1
1.9	0.0307	Sterol O-acyltransferase 1	Soat1
1.9	0.0264	cell division cycle associated 8	Cdca8
1.8	0.0212	budding uninhibited by benzimidazoles 1 homolog (S. cerevisiae)	Bub1
1.8	0.0119	regulator of G-protein signaling 16	Rgs16
1.8	0.0382	cyclin A2	Ccna2
1.8	0.0304	melanoma associated antigen (mutated) 1-like 1	Mum1l1
1.8	0.000652	FXYD domain-containing ion transport regulator 3	Fxyd3
1.8	0.0253	kinesin family member 20A	Kif20a
1.8	0.00912	"upstream binding transcription factor, RNA polymerase I"	Ubtf
1.8	0.0422	"Histone 1, H3i"	Hist1h3i
1.8	0.0115	aminoadipate-semialdehyde synthase	Aass
1.8	0.038	regulator of G-protein signaling 16	Rgs16

1.7	0.0169	RNA binding motif protein 14	Rbm14
1.7	0.0256	mucosal vascular addressin cell adhesion molecule 1	Madcam1
1.7	0.0238	RIKEN cDNA 2810417H13 gene	2810417H13Rik
1.7	0.0322	ubiquitin-conjugating enzyme E2C	Ube2c
1.7	0.0489	Shc SH2-domain binding protein 1	Shcbp1
1.7	0.013	"angiotensinogen (serpin peptidase inhibitor, clade A, member 8)"	Agt
1.7	0.0454	thioredoxin interacting protein	Txnip
1.7	0.00135	nitric oxide synthase trafficker	Nostrin
1.7	0.0186	estrogen-related receptor gamma	Esrrg
1.7	0.00517	"malic enzyme 3, NADP(+)-dependent, mitochondrial"	Me3
1.6	0.0256	RIKEN cDNA 1110064P04 gene	1110064P04Rik
1.6	0.011	centromere protein E	Cenpe
1.6	0.0126	zinc finger and BTB domain containing 16	Zbtb16
1.6	0.0136	"DNA segment, Chr 17, human D6S56E 5"	D17H6S56E-5
1.6	0.0107	protein C	Proc
1.6	0.0389	thyroid hormone receptor interactor 13	Trip13
1.6	0.0115	RIKEN cDNA 4632411J06 gene	4632411J06Rik
1.6	0.00872	thioredoxin interacting protein	Txnip
1.6	0.035	CD44 antigen	Cd44
1.6	0.00834	"cysteine and histidine-rich domain (CHORD)-containing, zinc-binding protein 1"	Chordc1
1.6	0.00406	myosin XVB	Myo15b
1.6	0.0332	RAS-related C3 botulinum substrate 2	Rac2
1.6	0.00409	baculoviral IAP repeat-containing 5	Birc5
1.6	0.0449	RIKEN cDNA 1200016G03 gene	1200016G03Rik
1.6	0.0232	fidgetin-like 1	Fignl1
1.6	0.0348	RIKEN cDNA 1700022C02 gene	1700022C02Rik
1.5	0.00722	SMC2 structural maintenance of chromosomes 2-like 1	Smc2l1
1.5	0.00127	Mohawk	Mkx
1.5	0.0418	RIKEN cDNA 4632411J06 gene	4632411J06Rik
1.5	0.0373	relaxin/insulin-like family peptide receptor 2	Rxfp2
1.5	0.0194	RNA binding motif protein 14	Rbm14
1.5	0.0116	Hemochromatosis	Hfe
1.5	0.00648	nudix(nucleoside diphosphate linked moiety X)type motif4	Nudt4
1.5	0.0243	thrombospondin 1 /// similar to thrombospondin 1	Thbs1 //LOC640441

Fold Decrease	*P-value*	*Gene title*	*Gene name*
3.3	0.00228	RIKEN cDNA 1100001E04 gene	1100001E04Rik
3.0	0.0208	glutamic acid decarboxylase 1	Gad1
2.7	0.0111	par6 partitioning defective 6 homolog γ (C. elegans)	Pard6g
2.7	0.0457	glutamic acid decarboxylase 1	Gad1
2.4	0.0262	cerebellin 4 precursor protein	Cbln4
2.2	0.0162	protocadherin 8	Pcdh8
2.2	0.000536	RIKEN cDNA 2210019I11 gene	2210019I11Rik
2.2	0.0339	aminolevulinic acid synthase 2, erythroid	Alas2
2.2	0.00775	RAB3C, member RAS oncogene family	Rab3c
2.2	0.0322	leucine-rich repeat LGI family, member 1	Lgi1
2.1	0.0177	Transcribed locus	---
2.0	0.000123	RAB3C, member RAS oncogene family	Rab3c
1.9	0.0112	nicotinamide nucleotide adenylyltransferase 2	Nmnat2
1.9	0.0482	hypothetical protein A230106N23	A230106N23
1.8	0.0087	expressed sequence AI428795	AI428795
1.8	0.0185	angiopoietin-like 7	Angptl7
1.8	0.0393	RIKEN cDNA A830010M20 gene	A830010M20Rik
1.8	0.00221	double C2, beta	Doc2b
1.8	7.82E-05	RIKEN cDNA 2300002D11 gene	2300002D11Rik
1.8	0.00523	cDNA sequence AB182283	AB182283
1.8	0.0234	transient receptor potential cation channel, subfamily M, member 5	Trpm5
1.7	0.0054	polo-like kinase 3 (Drosophila)	Plk3
1.7	0.0314	eyes absent 1 homolog (Drosophila)	Eya1
1.7	0.00572	transient receptor potential cation channel, subfamily M, member 5	Trpm5
1.7	0.0383	nuclear transcription factor, X-box binding 1	Nfx1
1.7	0.0395	solute carrier family 29 (nucleoside transporters), 4	Slc29a4
1.7	0.0466	CEA-related cell adhesion molecule 10	Ceacam10
1.7	0.0438	protocadherin alpha 1/ 2/ 3/ 4/ 5/ 6/ 7/ 8/ 9/ 10/ 11/ 12/ subfamily C, 1 / subfamily C, 2	Pcdha4/ 2/ 3/ 4/ 5/ 6/ 7/ 8/ 9/ 10/ 11/ 12// Pcdhac1/ 2
1.7	0.0433	receptor accessory protein 1	Reep1
1.7	0.0359	expressed sequence AW146242	AW146242
1.7	0.00376	RAS protein-specific guanine nucleotide-releasing factor 1	Rasgrf1
1.7	0.000447	glucagon receptor	Gcgr
1.6	0.0391	dual specificity phosphatase 26 (putative)	Dusp26
1.6	0.00487	F-box and leucine-rich repeat protein 10	Fbxl10
1.6	0.0149	RIKEN cDNA 1500005I02 gene	1500005I02Rik

1.6	0.0092	SEC14-like 1 (S. cerevisiae)	Sec14l1
1.6	0.0142	high mobility group box 3	Hmgb3
1.6	0.00899	leucine-rich repeat LGI family, member 1	Lgi1
1.6	0.0291	cDNA sequence BC020077	BC020077
1.6	0.0156	tubulin, beta 3	Tubb3
1.6	0.0191	RAS protein-specific guanine nucleotide-releasing factor 1	Rasgrf1
1.6	0.0338	RIKEN cDNA 2310028N02 gene	2310028N02Rik
1.6	1.31E-05	latrophilin 3	Lphn3
1.6	0.0384	RIKEN cDNA 6330500D04 gene	6330500D04Rik
1.6	0.0443	RIKEN cDNA 6720475J19 gene /// similar to putative retrovirus-related gag protein	6720475J19Rik /// LOC670480
1.6	0.0339	solute carrier family 39 (metal ion transporter), 8	Slc39a8
1.6	0.0226	acyl-CoA thioesterase 7	Acot7
1.6	0.0197	Adult male corpora quadrigemina cDNA, RIKEN full-length enriched library, clone:B230347A18	---
1.6	0.0298	cDNA sequence BC039632	BC039632
1.5	0.00205	Transcribed locus, moderately similar to XP_574723.1 PREDICTED: similar to LRRGT00097	---
1.5	0.0448	Vac14 homolog (S. cerevisiae)	Vac14
1.5	0.0327	expressed sequence AI428795	AI428795
1.5	0.0478	expressed sequence AI428795	AI428795
1.5	0.026	ciliary neurotrophic factor /// zinc finger protein 91	Cntf /// Zfp91
1.5	0.0256	immunoglobulin superfamily, member 4A	Igsf4a
1.5	0.0385	brachyury 2	T2

Supplemental Figure S1. Schematic of a $P2X_2$ current transient recorded from a *Sox4wt* β-cell expressing ionotropic $P2X_2$ receptors infused with 2 µM free $[Ca^{2+}]_i$ illustrating how the rise time ($t_{10\text{-}90\%;}$ time required for the current to increase from 10% to 90% of the peak amplitude), the half-width (the period that the amplitude exceeds 50% of the peak) and the charge (stippled area) were determined. The dotted vertical lines indicate the traces point at 10% and 90% of the maximal amplitude.

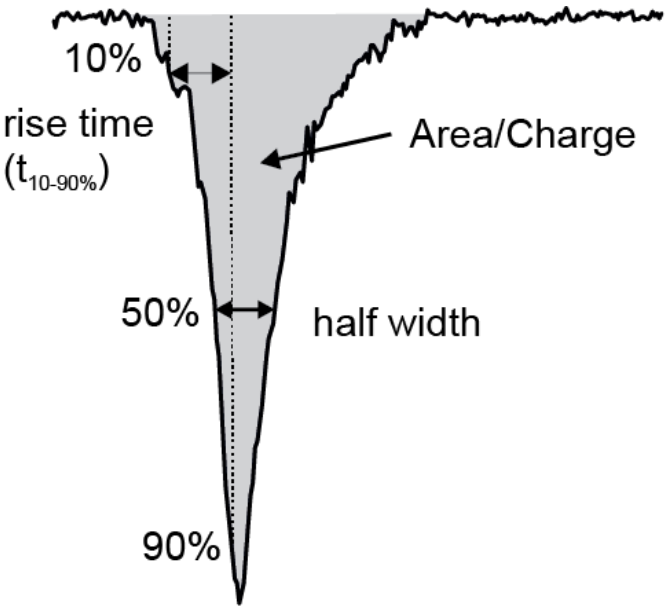

Supplemental Figure S2. Expression of *SOX4* in INS-1 832/13 cells following transfection with wild-type and mutant *Sox4*.

Sox4 expression was assessed in INS-1 832/13 cells transfected with scrambled siRNA + wtSox4 + hGH ('+Sox4') or scrambled siRNA + Sox4mt + hGH ('+Sox4mt'). Expression was normalised to that in cells expressing scrambled siRNA, DsRed and hGH (control).

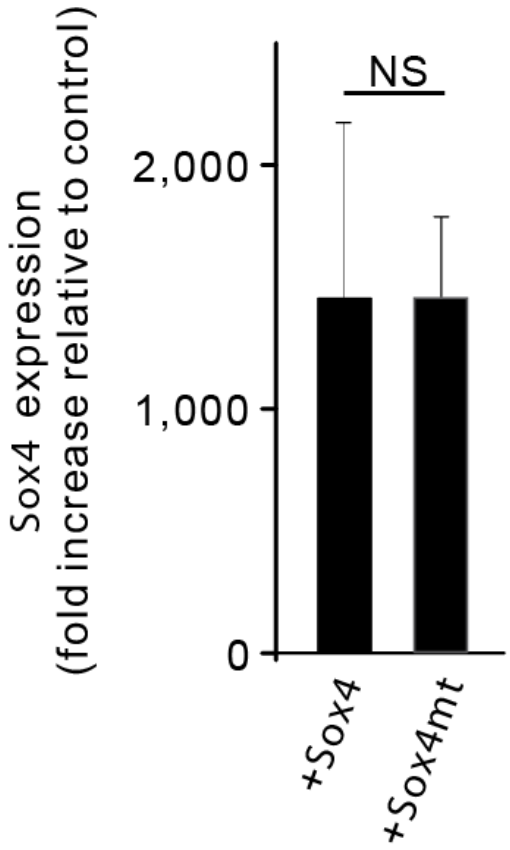

Supplemental Figure S3. Gene expression in human islets and insulin secretion in human β-cell line.

A: SOX4 expression in islets from non-diabetic (ND) and type-2 diabetic (T2D) organ donors. Values are presented as mean ± S.E.M.; n=31 for ND donors and n=21 for T2D donors. *B:* Relationship between CDKAL1 and SOX4 expression. R=0.191; *P*=0.036. For display, data have been grouped in quintiles. Best-fit black line represents Pearson correlation analysis to the individual data points. *C:* Insulin secretion in untransfected EndoC-βH2 cells exposed to 1 and 20 mM glucose. Mean ± S.E.M. of 3 experiments. *P<0.05 for the indicated comparisons. *D:* qRT PCR expression of exocytotic proteins (SNAP25, VAMP2 and STX1A (syntaxin-1A)) in control (black; scrambled siRNA + DsRed + hGH) and SOX4-overexpressing (red; scrambled siRNA + wtSOX4 + hGH) EndoC-βH2 cells. Data are presented as mean ± S.E.M. of 3 experiments, each with 3 replicates; *P<0.01 and ***P<0.001 for the indicated comparisons.

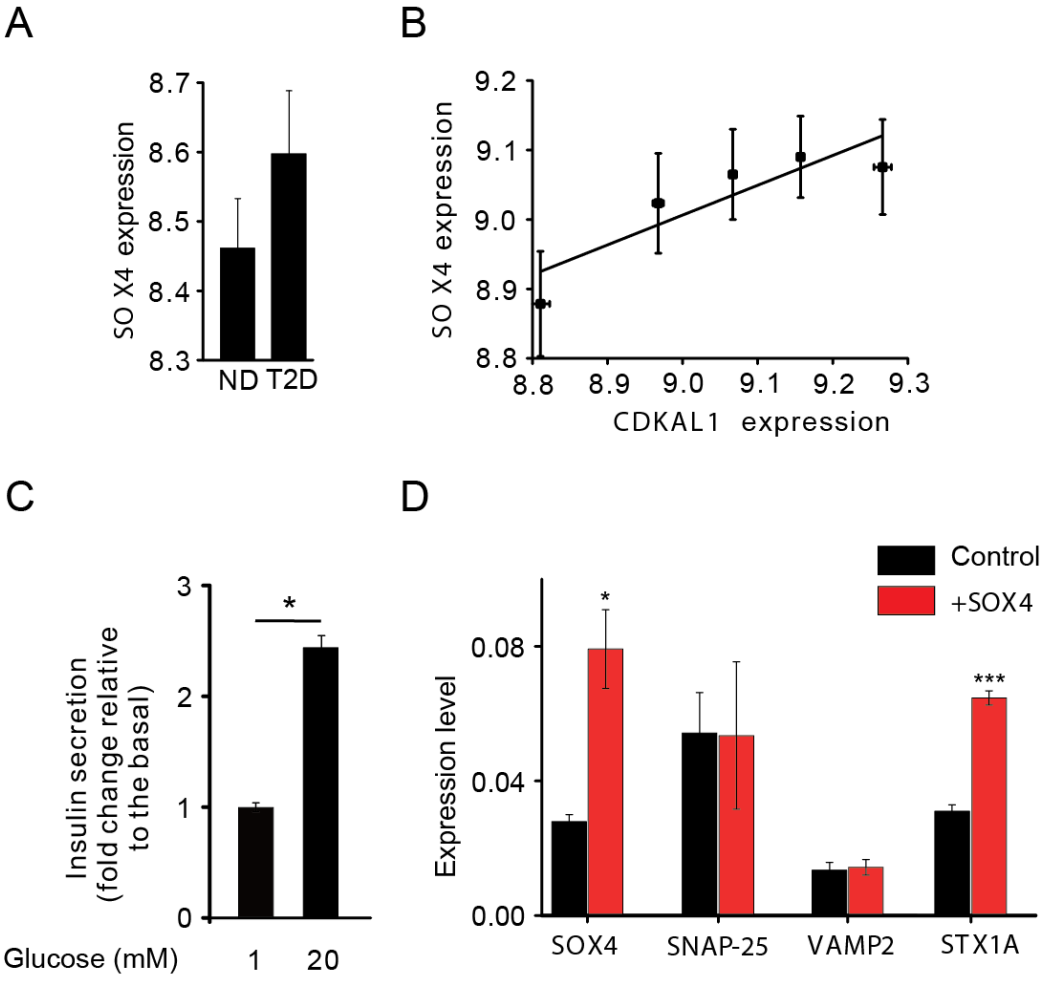

Supplemental Figure S4.

Schematic explaining the relationship between *STXBP6* expression, fusion pore opening and ATP/insulin release. When STXBP6 is expressed at low levels (i.e. Sox4wt cells; bottom), full fusion (top) associated with the rapid release of both ATP and insulin is the predominant form of exocytosis, giving rise to sharp spikes of ATP release detected by the PxX2R-based assay (middle).

A moderate increase in *STXBP6* expression (as seen in *Sox4mt* mice) stabilizes the fusion pore and delays/prevents its full opening in 50% of cases. Insulin is too bulky to be released via the fusion pore and its release depends on the eventual expansion of the fusion pore (if it occurs at all). However, ATP is small enough to exit via the fusion pore, giving rise to elongated spikes.

Strong overexpression of STXBP86 (as exemplified in the EndoC βH2 cells transfected with *STXBP6*) prevents fusion pore expansion and for the granules affected, the fusion pore will only partially and transiently open, giving rise to short-lived bouts of ATP release, before returning to the closed state. Under these conditions, insulin will not be released, explaining the strong suppression of hormone release observed.